

# Clockwise stellar disk and the dark mass in the Galactic Center

Andrei M. Beloborodov<sup>1,2</sup>, Yuri Levin<sup>3</sup>, Frank Eisenhauer<sup>4</sup>, Reinhard Genzel<sup>4,5</sup>, Thibaut Paumard<sup>4</sup>, Stefan Gillessen<sup>4</sup>, Thomas Ott<sup>4</sup>

## ABSTRACT

Two disks of young stars have recently been discovered in the Galactic Center. The disks are rotating in the gravitational field of the central black hole at radii  $r \sim 0.1 - 0.3$  pc and thus open a new opportunity to measure the central mass. We find that the observed motion of stars in the clockwise disk implies  $M = (4.3 \pm 0.5) \times 10^6 M_\odot$  for the fiducial distance to the Galactic Center  $R_0 = 8$  kpc and derive the scaling of  $M$  with  $R_0$ . As a tool for our estimate we use orbital roulette, a recently developed method. The method reconstructs the three-dimensional orbits of the disk stars and checks the randomness of their orbital phases. We also estimate the three-dimensional positions and orbital eccentricities of the clockwise-disk stars.

*Subject headings:* Galaxy: center — galaxies: general — stellar dynamics

## 1. INTRODUCTION

A supermassive black hole is believed to reside in the dynamical center of the Galaxy (Eckart & Genzel 1996; Genzel et al. 1997; Ghez et al. 1998; Schödel et al. 2002; Genzel et al. 2000; Ghez et al. 2000; Schödel et al. 2003; Ghez et al. 2003). It is associated with the compact radio source Sgr A\* and dominates the gravitational potential at distances  $r < 1$  pc from the center. The central mass has been estimated with a few different methods. In particular, the statistical analysis of sky-projected positions and velocities of stars in the central 0.5 pc gave estimates that range above  $3 \times 10^6 M_\odot$  (Genzel et al. 2000; Schödel et al. 2003). The systematic error of these estimates, however, is difficult to quantify as they depend on the assumed three-dimensional statistical model of the cluster.

Independent estimates of the black hole mass were derived from observations of a few stars (S-stars) that move on very tight orbits around Sgr A\* , at radii  $r \sim 0.01$  pc, and have orbital

---

<sup>1</sup>Physics Department and Columbia Astrophysics Laboratory, Columbia University, 538 West 120th Street New York, NY 10027

<sup>2</sup>Astro-Space Center of Lebedev Physical Institute, Profsojuznaja 84/32, Moscow 117810, Russia

<sup>3</sup>Leiden Observatory, PO Box 9513, NL-2300 RA, Leiden, The Netherlands

<sup>4</sup>Max-Planck Institut für extraterrestrische Physik (MPE), Garching, Germany

<sup>5</sup>Department of Physics, University of California, Berkeley, CA 94720

periods as short as a few decades. Fractions of S-star orbits have been mapped out over the past decade (Schödel et al. 2002; Schödel et al. 2003; Ghez et al. 2003; Ghez et al. 2005). By checking which value of the central mass provides an acceptable fit to the orbital data, Eisenhauer et al. (2005) found  $M = (4.1 \pm 0.4) \times 10^6 M_\odot$ , and Ghez et al. (2005) found  $M = (3.7 \pm 0.2) \times 10^6 M_\odot$  for the fiducial distance to the Galactic Center  $R_0 = 8$  kpc. Same star orbits were used to derive  $R_0 = 7.62 \pm 0.32$  kpc (Eisenhauer et al. 2005), in agreement with previous methods (e.g. Reid et al. 1993).

In this paper, we report a new independent estimate of the central mass that uses the young massive stars at  $r \sim 0.1 - 0.3$  pc as test particles. A remarkable property of these stars has been discovered recently: they form a disk-like population (Levin & Beloborodov 2003; Genzel et al. 2003). Two stellar disks apparently coexist at these radii. One of them rotates clockwise on the sky and the other one — counter-clockwise. New observations of Paumard et al. (2006) have increased the number of known disk members by a factor of three and show clearly the two-disk structure of the young population. The clockwise disk is especially well pronounced. It has about 30 members and a small thickness  $H/r \approx 0.1$ .

In this paper, we investigate the orbital motions of stars in the clockwise disk and infer the central gravitating mass. As a tool of our mass estimate we use orbital roulette, a recently developed statistical method (Beloborodov & Levin 2004, hereafter BL04). This method is generally more precise than the estimators based on the virial theorem and provides a statistically well-defined way to quantify the uncertainty of the mass estimate.

## 2. CLOCKWISE DISK

The disk-like structure of the young stellar population is not evident when it is observed in projection: the line-of-sight coordinates  $z$  of the stars are unknown. This structure, however, is evident in the distribution of the measured 3D velocities. In particular, the velocity vectors of stars that move clockwise on the sky cluster near a particular plane. This may be only if the orbits of stars are near this plane and form a disk-like population.

The clockwise disk has a small thickness at angular distances  $0.7'' < d < 5''$  from Sgr A\* . We use the stars in this region to define the midplane of the disk. It is defined as the midplane of the observed velocity vectors, and its normal vector is<sup>1</sup>  $\mathbf{n}_0 = (-0.135, -0.857, 0.497)$ . The deviations of individual stellar velocities from the midplane are shown in Figure 1. Hereafter in this paper we use the sample of stars between  $0.7''$  and  $5''$  with firmly detected clockwise rotation  $l_z = xv_y - yv_x > 2\Delta l_z$ , where  $\Delta l_z$  is the measurement error in  $l_z$ .

---

<sup>1</sup> $(x, y, z)$  are standard coordinates: they are chosen so that Sgr A\* is at the origin, the  $x$  and  $y$  axes are in the plane of the sky and directed along increasing right ascension and declination, respectively, and the  $z$  axis is directed along the line of sight away from us.

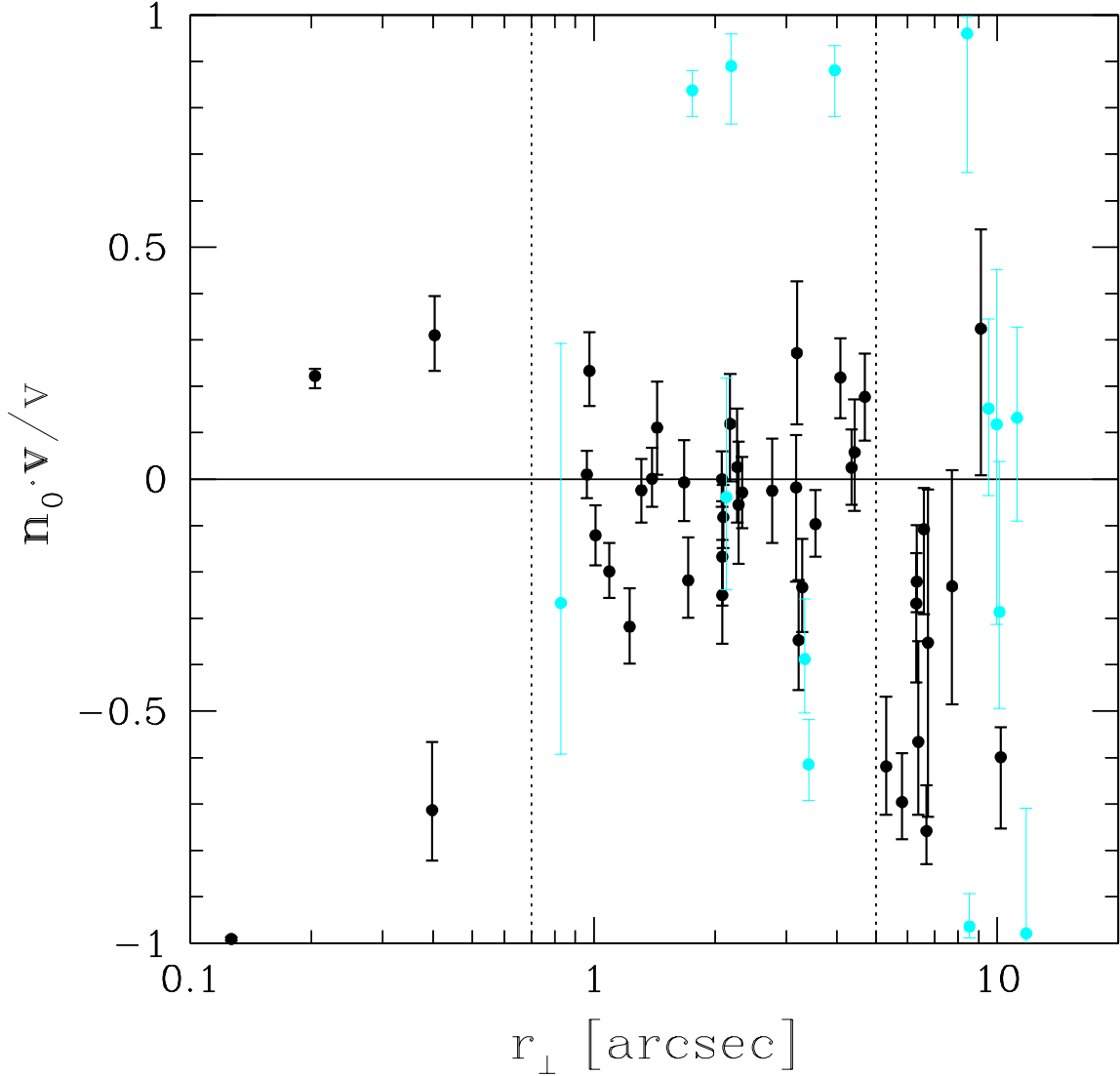


Fig. 1.— Quantity  $\mu = \mathbf{n}_0 \cdot \mathbf{v} / v$  for all young stars observed by Paumard et al. (2006) that have apparent clockwise rotation on the sky  $l_z > 0$ , shown versus projected distance from Sgr A\* . For randomly oriented orbits,  $\mu$  would be uniformly distributed between  $-1$  and  $1$ . The actual data show a strong clustering around  $\mu = 0$  (midplane). Data shown in black represent the stars with firmly detected clockwise rotation  $l_z > 2\Delta l_z$ , and cyan points — the stars with  $0 < l_z < 2\Delta l_z$ , where  $\Delta l_z$  is the error in  $l_z$ . The sample used in this paper is the 28 stars shown in black in the region  $0.7'' < r_{\perp} < 5''$ .

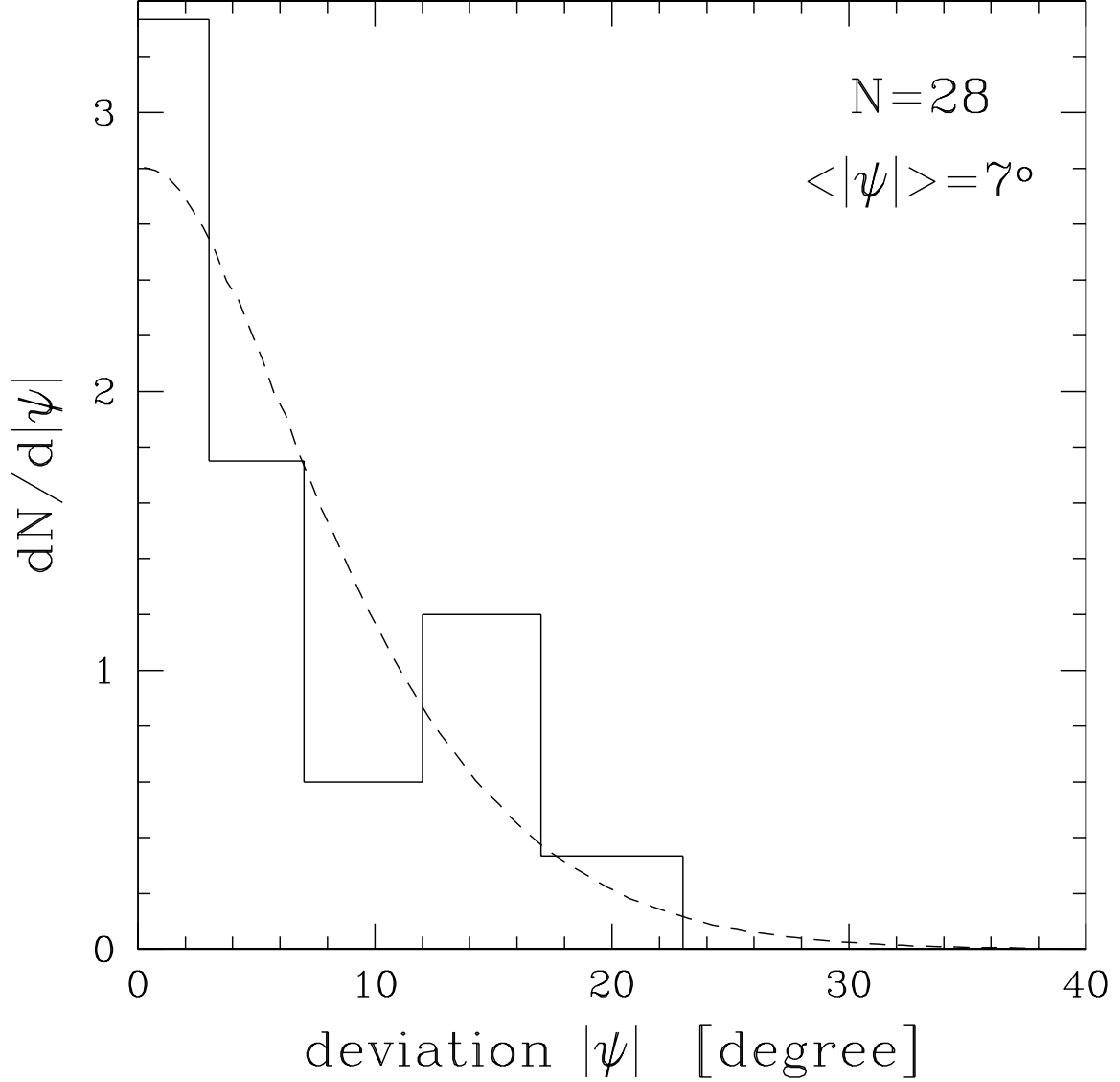


Fig. 2.— Histogram of the angles  $\psi_i$  between observed best-fit velocities  $\mathbf{v}_i$  and the disk midplane with normal  $\mathbf{n}_0$ . Angle  $\psi$  is related to  $\mu$  shown in Figure 1 by  $\sin \psi = \mu$ . The mean value of  $|\psi|$  is  $\langle |\psi| \rangle = 7.1^\circ$  and  $\langle \psi^2 \rangle^{1/2} = 9.3^\circ$ . Dashed curve shows the distribution of  $|\psi|$  expected from our model disk population. The dispersion of orbital inclinations  $\theta$  in the model is  $10^\circ$ .

## 2.1. Thickness of the Disk

The sample has 28 stars, which is sufficiently large to study the distribution of velocity deviations from the disk midplane (Fig. 2). The deviation angles  $\psi_i$  are defined by  $\psi_i = \arcsin(\mathbf{n}_0 \cdot \mathbf{v}_i / v_i)$ . The observed distribution of  $\psi$  may be fitted by a disk population model. We will use a simple Gaussian model of orbital inclinations  $\theta$  around the midplane. The probability distribution of  $\theta$  is then given by  $P(\theta) = (2/\pi)^{1/2}(\Delta\theta)^{-1} \exp[-(\theta/\Delta\theta)^2/2]$ .

The Gaussian model of the disk has one parameter — the dispersion  $\Delta\theta$  — and predicts a certain probability distribution for  $\psi$ . We calculate this distribution using Monte-Carlo technique, including a simulation of observational errors. We randomly draw  $N = 28$  orbits from the model population and choose a randomly directed vector of length  $v_i$  in each orbital plane  $i = 1, \dots, N$ . This gives 28 simulated velocities  $\mathbf{v}_i$ . Then observational errors  $\Delta\mathbf{v}_i$  are added to each  $\mathbf{v}_i$  (the real  $v_i$  and  $\Delta\mathbf{v}_i$  from Paumard et al. 2006 are used). Finally, deviations  $\psi_i$  of velocities  $\mathbf{v}_i$  from the disk midplane are calculated. This simulation is repeated  $10^5$  times, which gives the accurate distribution of  $\psi$  predicted by the model as well as the average values  $\langle|\psi|\rangle$  and  $\langle\psi^2\rangle^{1/2}$  as functions of  $\Delta\theta$ .

The observed  $\langle|\psi|\rangle \approx 7^\circ$  and  $\langle\psi^2\rangle^{1/2} \approx 9^\circ$  are reproduced by the Monte-Carlo model with  $\Delta\theta \approx 10^\circ$ . The model is consistent with the observed distribution of  $\psi$  for  $\Delta\theta = 10 \pm 3^\circ$ . Hereafter we will use the best-fit model with  $\Delta\theta = 10^\circ$ .

The geometrical thickness of the disk may be described by the elevation of stars above/below the midplane,

$$\frac{H}{r} = |\sin \phi \sin \theta|, \quad (1)$$

where  $\phi$  is the orbital phase of the star, and  $\theta$  is the inclination of its orbit. Assuming circular orbits for simplicity, one finds after averaging over the orbital phase,

$$\frac{H}{r} = \left(\frac{2}{\pi}\right)^{1/2} \langle \sin \theta \rangle. \quad (2)$$

This gives for the Gaussian model (approximating  $\sin\langle\theta\rangle \approx \langle\sin\theta\rangle$  for small  $\Delta\theta = 0.17$ ),

$$\frac{H}{r} = \left(\frac{2}{\pi}\right)^{3/2} \sin \Delta\theta = 0.09 \pm 0.03. \quad (3)$$

## 2.2. Circular Motion?

We now check whether the data is consistent with circular motion of the disk stars. The assumption of circular motion implies that radius-vector  $\mathbf{r}_i$  of the  $i$ -th star satisfies

$$\mathbf{r}_i^{\text{cir}} \cdot \mathbf{v}_i = 0, \quad i = 1, \dots, N. \quad (4)$$

This equation, together with the known position  $(x_i, y_i)$  on the sky, determines  $z_i$  — the line-of-sight coordinate of the star. The easiest way to test the circular-motion hypothesis is to look at the orientations of orbital planes implied by this hypothesis. The inferred  $\mathbf{r}_i^{\text{cir}}$  allow us to calculate the angular momentum vector for each star

$$\mathbf{l}_i^{\text{cir}} = \mathbf{r}_i^{\text{cir}} \times \mathbf{v}_i, \quad i = 1, \dots, N, \quad (5)$$

and then find its deviation  $\theta_i^{\text{cir}}$  from the disk axis  $\mathbf{n}_0$ . The dispersion of  $\theta_i^{\text{cir}}$  would be expected to be consistent with dispersion  $\Delta\theta \approx 10^\circ$  of orbital planes inferred directly from  $\mathbf{v}_i$ . The actual distribution of  $\theta_i^{\text{cir}}$  is shown in Figure 3. One can see that the circular hypothesis implies orbital inclinations that are inconsistent with the found thickness of the disk. A significant fraction of the disk stars must have non-negligible eccentricities.

A circular orbit would provide a straightforward estimate of the central mass  $M$ . Indeed, circular motion implies a simple relation between  $M$ ,  $v$ , and  $r$ :  $GM = rv^2$ . An estimate of  $M$  could be done by applying this relation to stars with small  $\theta^{\text{cir}}$ , which are possibly on circular orbits. However, it is difficult to quantify the accuracy of such analysis. A more accurate estimate of  $M$  is made in § 4, without making any prior assumptions on eccentricities.

### 2.3. Three-Dimensional Positions

Measurements of stellar positions relative to Sgr A\* are limited to 2 dimensions — the plane of the sky. However, the stars that belong to the clockwise disk have an extra constraint on their 3D positions  $\mathbf{r}_i$ : they must be close to the midplane of the stellar disk. This constraint may be written as

$$(\mathbf{n}_0 \pm \Delta\mathbf{n}) \cdot \mathbf{r}_i = 0, \quad i = 1, \dots, N, \quad (6)$$

where  $\mathbf{n}_0$  is the disk axis and  $\Delta\mathbf{n}$  represents the dispersion of orbital planes around the disk midplane.

The line-of-sight coordinate of the  $i$ -th star is then given by

$$z_i = -\frac{x_i n_{x,i} + y_i n_{y,i}}{n_{z,i}}, \quad \mathbf{n}_i = \mathbf{n}_0 \pm \Delta\mathbf{n}. \quad (7)$$

The orbital plane  $\mathbf{n}_i$  may differ from the best-fit disk plane by  $\sim 10^\circ$ , which induces an error in the inferred  $z$ -coordinate. To estimate the error we rock  $\mathbf{n}_i$  with a Gaussian distribution around  $\mathbf{n}_0$  with a mean deviation of  $10^\circ$ .

The resulting  $z_i$  and their uncertainties are found using the following Monte-Carlo simulation. We draw randomly  $\mathbf{n}_i$  and  $v_{x,i}$ ,  $v_{y,i}$  from their measured Gaussian distributions. Then we determine  $v_{z,i}$  from the condition  $\mathbf{v}_i \cdot \mathbf{n}_i = 0$ . The obtained realization of  $\mathbf{n}_i$  and  $\mathbf{v}_i$  is given a weight that corresponds to the level of consistency of  $v_{z,i}$  with the measured Gaussian  $v_{z,i} = v_{z,i} \pm \Delta v_{z,i}$ . (In the simulation, we get this weight by rejecting the realization if its  $v_{z,i}$  is farther in the Gaussian

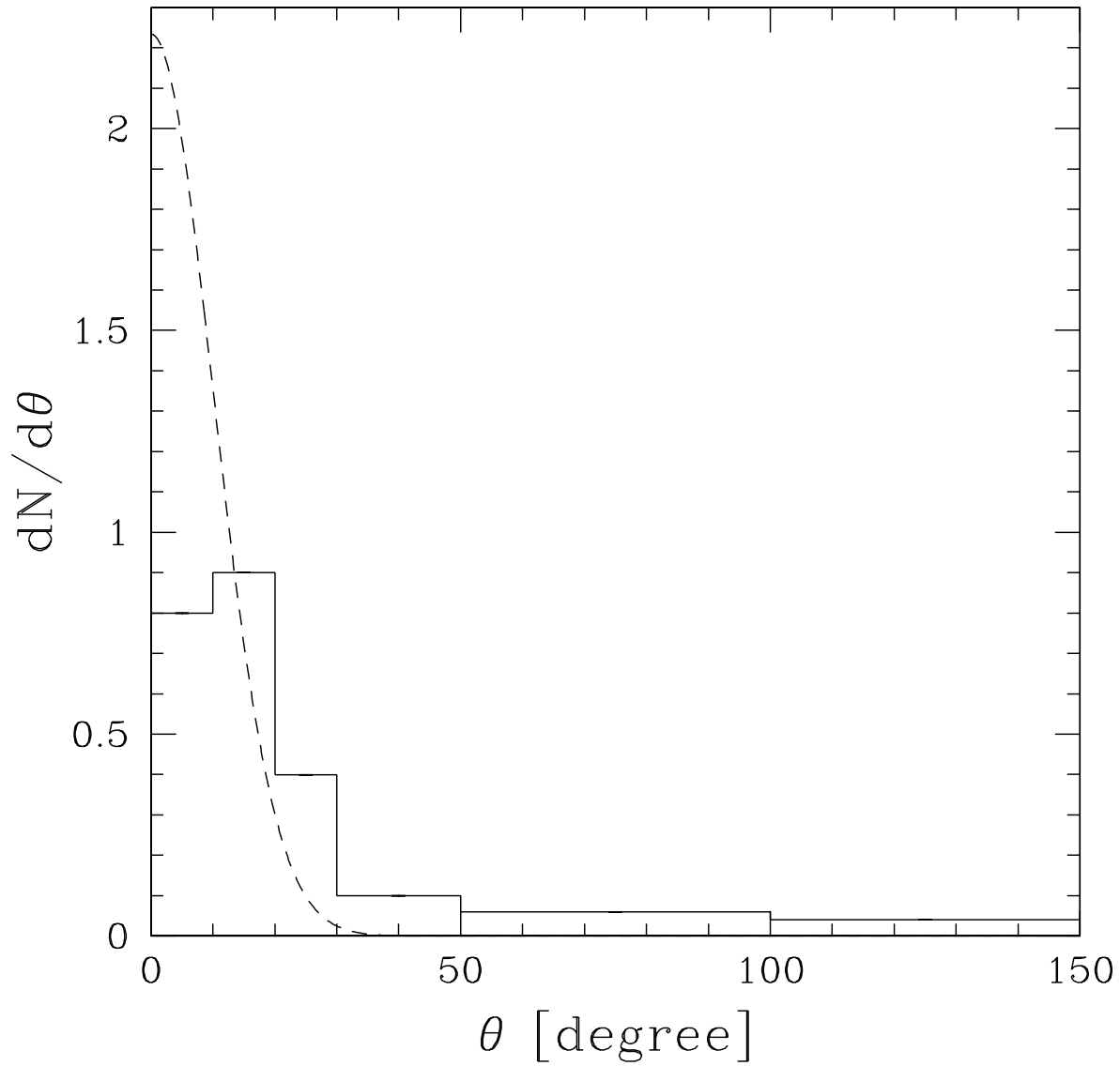


Fig. 3.— Histogram of orbital inclinations  $\theta$  that would be inferred from the circular hypothesis. Dashed curve shows the  $10^\circ$  Gaussian distribution of  $\theta$  that fits the 3D velocity data (see Fig. 2). The circular hypothesis implies large orbital inclinations  $\theta > 30^\circ$  for at least 1/4 of stars, which is inconsistent with the observed narrow distribution of velocity angles  $\psi_i$ .

tail than a randomly chosen  $v'_{z,i}$  from the Gaussian distribution.) In this way, a realization  $\mathbf{n}_i, \mathbf{v}_i$  is given the weight that takes into account both the thickness of the disk and the error of the 3D velocity. We find the mean  $z_i$  and its dispersion  $\Delta z_i$  using about  $10^6$  realizations.

The deduced 3D positions together with the measured 3D velocities give 6D information for each star. Then the velocities  $v_r$  and  $v_\phi$  may be deduced, where  $r$  and  $\phi$  are polar coordinates in the orbital plane of the star. The measurement errors of  $\mathbf{v}_i$  and the uncertainty in the individual orbital planes imply errors  $\Delta v_r$  and  $\Delta v_\phi$ . We estimate the uncertainties assuming the Gaussian dispersion in  $\mathbf{n}_i$  with  $\Delta\theta = 10^\circ$  and Gaussian velocity errors  $\Delta\mathbf{v}_i$ . The results are summarized in Table 1 and illustrated in Figure 4.

### 3. MASS ESTIMATION USING ORBITAL ROULETTE

The orbital periods of stars at  $r \gtrsim 0.1$  pc are thousands of years, and it is presently impossible to trace any significant fraction of the orbits. Therefore, a statistical method must be applied using the observed *instantaneous* positions  $\mathbf{r}_i$  and velocities  $\mathbf{v}_i$  of the stars. Such a method must take into account the possible errors in  $\mathbf{r}_i$  and  $\mathbf{v}_i$ .

A traditional mass estimate would be based on the virial theorem,

$$M = \frac{\sum v_i^2}{G \sum 1/r_i}. \quad (8)$$

The virial relation gives  $M = 3.8 \times 10^6 M_\odot$ . One faces difficulties, however, when trying to define the error of this estimate (see BL04 for discussion).

A major assumption in the derivation of the virial relation (8) is that the stars have random orbital phases. BL04 have shown that the random-phase (“roulette”) principle can be applied directly to data, without invoking the virial theorem, and this gives a more accurate and statistically complete estimator. It judges any trial gravitational potential  $\Phi(r)$  by reconstructing the orbits in this potential and checking the inferred orbital time phases. The true potential must give a “fair roulette” — a random (flat) distribution of the phases.

The 3D positions of the disk stars have uncertainties because their precise orbital planes are unknown. Besides, the 3D velocities are measured with errors. We take into account the uncertainties using Monte-Carlo technique: many random realizations of the data set  $(\mathbf{r}_i, \mathbf{v}_i)$  are generated and studied. The possible  $(\mathbf{r}_i, \mathbf{v}_i)$  are generated assuming the  $10^\circ$  Gaussian distribution of the orbital planes and Gaussian errors in  $\mathbf{v}_i$  with dispersions  $\Delta\mathbf{v}_i$  given in Paumard et al. (2006).

Each realization of the data set  $(\mathbf{r}_i, \mathbf{v}_i)$  is analyzed by the roulette estimator as described in BL04. The analysis aims to accept or rule out a trial potential  $\Phi(r) = -GM_{\text{trial}}/r$  at a chosen confidence level. Given  $M_{\text{trial}}$  and a data set  $(\mathbf{r}_i, \mathbf{v}_i)$  one can reconstruct all  $N = 28$  orbits and find the time orbital phases  $g_i$  of the stars. The time phase  $g$  is defined so that  $g = 0$  at the pericenter of the orbit and  $g = 1$  at the apocenter. To judge  $M_{\text{trial}}$  we check the consistency of  $g_i$  with the



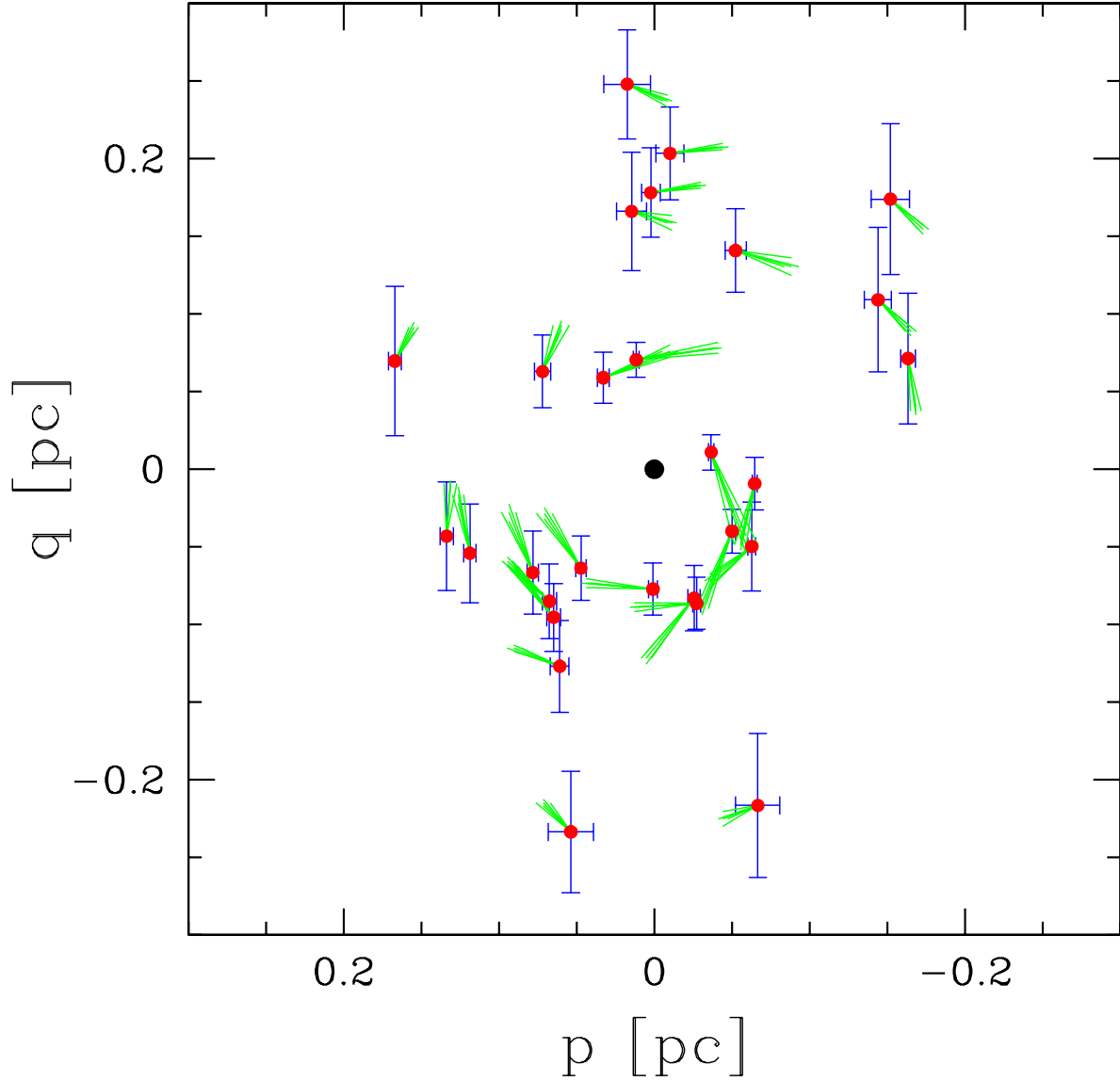


Fig. 4.— Positions and velocities of the 28 stars in the disk plane  $(p, q)$ . Sgr A\* is located at the origin (black circle). The  $p$ -axis is chosen in the intersection of the disk plane with the  $(x, z)$  plane and the  $q$ -axis is perpendicular to the  $p$ -axis. The axis directions (unit vectors)  $\mathbf{e}_p$  and  $\mathbf{e}_q$  are chosen so that  $\mathbf{e}_p \cdot \mathbf{e}_x > 0$  and  $\mathbf{e}_q \cdot \mathbf{e}_y > 0$ . The velocity of each star is shown by 5 vectors: the best-fit vector  $\mathbf{v}_i$ ,  $\mathbf{v}_i \pm \Delta v_p \mathbf{e}_p$ , and  $\mathbf{v}_i \pm \Delta v_q \mathbf{e}_q$ . We show the stars in a single plane, as if they had a common orbital plane. Their real orbits may differ from the disk midplane by  $\sim 10^\circ$ , and the corresponding uncertainties in positions are indicated in the figure. The distance to the Galactic Center  $R_0 = 8$  kpc is assumed.

expected flat distribution between 0 and 1 (and do that for many realizations of the data sets to take into account the uncertainties in the data).

The roulette algorithm is described in detail in BL04. Here we use its simplest version based on the analysis of the mean phase  $\bar{g} = N^{-1} \sum g_i$ . The true  $M$  must satisfy the condition

$$\bar{g}(M) = 0.5 \pm (12N)^{-1/2}. \quad (9)$$

If  $M_{\text{trial}}$  is too small then  $\bar{g}(M_{\text{trial}}) \rightarrow 0$ , i.e. all stars will be found near the pericenter, while too large  $M_{\text{trial}}$  will give  $\bar{g}(M_{\text{trial}}) \rightarrow 1$ , i.e. all stars will sit near apocenter. One can accept only such  $M_{\text{trial}}$  that give  $\bar{g}$  consistent with the fair roulette (eq. 9).

In our Monte-Carlo simulation,  $\bar{g}(M_{\text{trial}})$  that is found for a realization of the data set  $(\mathbf{r}_i, \mathbf{v}_i)$  is compared with  $\bar{g}'$  found for a realization of a fair roulette  $g'_i$ . The statistics of this comparison is accumulated for  $10^6$  random realizations. Thus, the probability  $P_-$  of  $\bar{g}(M_{\text{trial}}) < \bar{g}'$  is accurately found.

The probability  $P_-(M_{\text{trial}})$  is monotonically increasing with  $M_{\text{trial}}$  since larger masses imply larger orbital phases (closer to the apocenter). Trial masses that give small  $P_-$  are ruled out with significance  $P_-$  (BL04). If  $P_- > 1/2$ , we look at  $P_+ = 1 - P_-$ . Trial masses that give small  $P_+ < 1/2$  are ruled out with significance  $P_+$ .

The found functions  $P_{\pm}(M_{\text{trial}})$  are shown in Figure 5. The confidence intervals for  $M$  are between the two curves. For example, the 80% confidence interval ( $P_- = P_+ = 0.1$ ) is  $3.85 \times 10^6 M_{\odot} < M < 4.93 \times 10^6 M_{\odot}$ . The confidence intervals approximately correspond to a Gaussian distribution with standard deviation  $(0.4 - 0.5) \times 10^6 M_{\odot}$ , and we can summarize the result as  $M = (4.3_{-0.4}^{+0.5}) \times 10^6 M_{\odot}$ .

We have also checked the distribution of  $g_i$  for the found  $M$ . It is consistent with the expected flat distribution; this is verified using the Anderson-Darling measure (see BL04). We conclude that the observed stellar motions are consistent with Kepler potential  $\Phi = -GM/r$  with  $M = (4.3_{-0.4}^{+0.5}) \times 10^6 M_{\odot}$ .

There are two sources of systematic error of our result. First, we had to chose a disk-population model in the calculations. We specified the midplane (normal  $\mathbf{n}_0$ ) and the Gaussian distribution of orbital inclinations around the midplane with dispersion  $\Delta\theta$ . The parameters  $\mathbf{n}_0$  and  $\Delta\theta$  have been derived by fitting the 3D velocity data and have finite errors. The obtained  $M$  is most sensitive to  $n_{z0}$  which determines the disk inclination to the line of sight. Our best-fit disk has  $n_{z0} \approx 0.5$ ; larger  $n_z$  would imply smaller sizes of the orbits and hence smaller  $M$ .  $n_{z0}$  as large as 0.6 may still be consistent with the velocity data (Paumard et al. 2006), and it would change our estimate to  $M = (4.0_{-0.3}^{+0.5}) \times 10^6 M_{\odot}$ . The parameter  $\Delta\theta$  has the error of  $3^\circ - 4^\circ$ . The choice of  $\Delta\theta = 13^\circ$  instead of  $10^\circ$  would broaden the confidence intervals by a factor  $\sim 1.2$ .

The second possible source of error is the distance to the Galactic Center  $R_0$  which we assumed to be 8 kpc. The mass estimate depends on  $R_0$  because the proper velocities  $\mathbf{v}_{\perp} = (v_x, v_y)$  and

positions  $(x, y)$  scale linearly with  $R_0$  ( $v_z$  is not affected as its measurement is based on the Doppler effect). The midplane of the disk varies little and may be assumed constant to a first approximation. Then the deduced radial positions  $r$  of the stars scale linearly with  $R_0$ . The dependence of  $M$  on  $R_0$  may be derived using a toy problem with  $N \gg 1$  stars moving in the disk midplane on a circular orbit of radius  $r_{\text{true}}$ . The true and deduced masses are then given by

$$GM_{\text{true}} = r_{\text{true}} (v_{\perp, \text{true}}^2 + v_z^2),$$

$$GM = r (v_{\perp}^2 + v_z^2) = r_{\text{true}} \left( \frac{R_0}{R_{0\text{true}}} \right) \left[ v_{\perp, \text{true}}^2 \left( \frac{R_0}{R_{0\text{true}}} \right)^2 + v_z^2 \right].$$

After averaging over  $N$  stars and taking into account that  $\langle v_{\perp, \text{true}}/v_{\text{true}} \rangle = (1+n_z^2)/2$  and  $\langle v_z/v_{\text{true}} \rangle = (1-n_z^2)/2$ , we find

$$M(R_{0\text{true}}) = M(8 \text{ kpc}) \left[ \frac{1}{2}(1+n_z^2) \left( \frac{R_{0\text{true}}}{8 \text{ kpc}} \right)^{-3} + \frac{1}{2}(1-n_z^2) \left( \frac{R_{0\text{true}}}{8 \text{ kpc}} \right)^{-1} \right]^{-1}. \quad (10)$$

We have empirically checked this dependence by repeating the roulette simulation for various  $R_0$  (as small as 7 kpc). The obtained  $P_{\pm}(M)$  are well described by a simple shift of  $M$  according to equation (10). In particular,  $R_0 = 7.6$  kpc (Eisenhauer et al. 2005) would give  $M = (3.8_{-0.3}^{+0.4}) \times 10^6 M_{\odot}$ .

Table 1 shows the eccentricities of reconstructed star orbits for  $R_0 = 8$  kpc and the best-fit central mass  $M = 4.3 \times 10^6 M_{\odot}$ . The errors  $\Delta e_i$  ( $i = 1, \dots, 28$ ) are caused by uncertainties  $\Delta \mathbf{v}_i$  and  $\Delta \mathbf{n}_i$ . The errors are found using the Monte-Carlo simulation that is similar to the estimation of  $\Delta z_i$  (see § 2.3). This simulation gives the probability distribution  $f(e_i)$  for each  $e_i$ . A non-zero eccentricity is detected if  $\bar{e}_i > 2\Delta e_i$  and accurately measured if  $\bar{e}_i > 3\Delta e_i$ , where  $\bar{e}_i$  is the mean of  $f(e_i)$  and  $\Delta e_i$  is its dispersion. If distribution  $f(e_i)$  is broad (large errors), its mean represents the errors rather than the true  $e_i$ . Therefore,  $\bar{e}_i$  is an accurate estimate of eccentricity only if the distribution  $f(e_i)$  is sufficiently narrow,  $\Delta e_i \lesssim 0.3\bar{e}_i$ . Table 1 shows  $\bar{e}_i \pm \Delta e_i$  for stars with  $\Delta e_i < 0.5\bar{e}_i$ . For stars with  $\Delta e_i > 0.5\bar{e}_i$  we give  $\bar{e}_i + \Delta e_i$  as an upper limit. The obtained values are consistent with the results of Paumard et al. (2006) where eccentricities are estimated with another method.

#### 4. DISCUSSION

The reconstructed orbits of stars in the clockwise disk depend on the assumed central mass  $M$ . In particular, the star orbital phases depend on  $M$ . We have used this dependence to estimate  $M$ : the true  $M$  must give time phases consistent with a uniform distribution. This is the first practical application of orbital roulette, a new method of estimating the gravitational potential from instantaneous motions of test bodies (BL04).

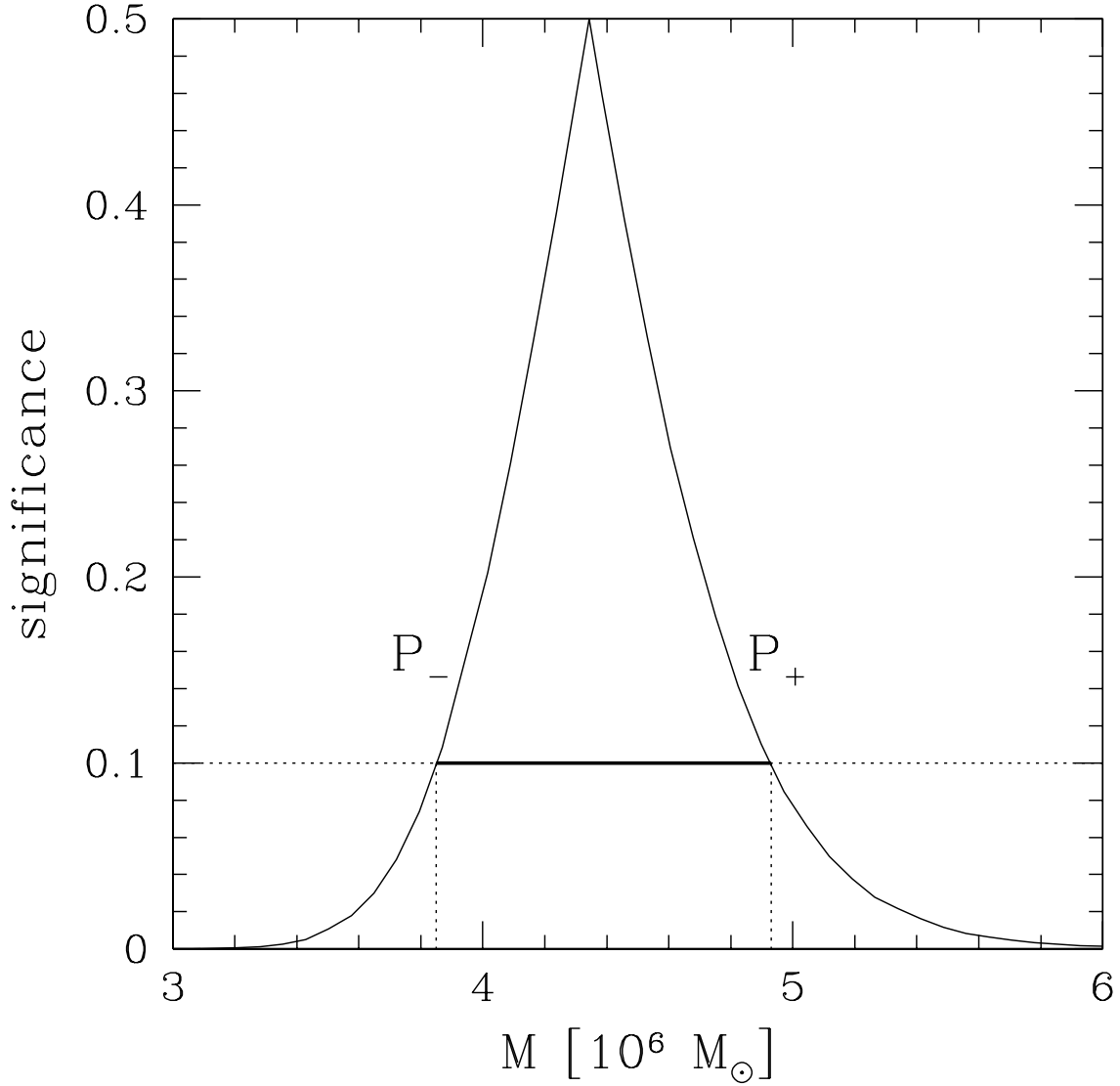


Fig. 5.— Confidence intervals for Sgr A\* mass  $M$  found with the roulette method. For example the 80% confidence interval ( $P_+ = P_- = 0.1$ ) is shown by the horizontal solid line ( $P_+ = P_- = 0.1$ ). The distance to the Galactic Center  $R_0 = 8$  kpc is assumed. The scaling of the estimated mass with  $R_0$  is given by eq. (10).

The obtained estimate  $M = (4.3_{-0.4}^{+0.5}) \times 10^6 M_\odot$  is consistent with the recent estimates based on the maps of orbits of S stars in the very vicinity of the center ( $r < 0.01$  pc). The independent estimate presented here uses different stars at  $r = 0.1 - 0.3$  pc and is complementary to the small-scale estimates. It measures the total mass within  $r \sim 0.1$  pc which may include stars and dark matter.

The approximate equality of the masses within the central 0.1 pc and 0.01 pc implies an upper bound on the mass between 0.01 and 0.1 pc:  $\Delta M \lesssim 0.5 \times 10^6 M_\odot$ . This constrains a possible cusp of the stellar population around the central black hole as well as the dark-matter content of the central region. Further observations may provide a better constraint or resolve  $\Delta M$ .

The data shows an inner cutoff of the disk population at a radius  $r \sim 0.05$  pc (see Fig. 1 and Paumard et al. 2006). The observed peak of the population at  $r \sim 0.1$  pc supports the hypothesis that the young stars were born in a gravitationally unstable accretion disk (LB03).

The found geometrical thickness of the clockwise stellar population  $H/r = 0.09 \pm 0.03$  (eq. 3) does not imply that it was born with this  $H/r$ . The parent accretion disk was likely thinner, and its stellar remnant have thickened with time. The age of the stellar population,  $t_{age} = (6 \pm 2)$  million years, should be compared with the timescale of diffusion of orbital parameters. The latter may be written as

$$t_{diff} \sim 0.1 \frac{v^3}{G^2 m_* \rho_* \ln(N_*/2)}, \quad (11)$$

where  $m_*$  is a characteristic mass of the objects that dominate fluctuations of the gravitational potential,  $\rho_*$  is their mass density averaged over the considered region  $r \sim 0.3$  pc, and  $N_* \sim (4\pi/3)r^3\rho_*/m_*$  is the total number of these objects. In a uniform stellar core of total mass  $\sim 3 \times 10^5 M_\odot$ , the fluctuations would be dominated by low-mass stars, whose total number is  $N_* \sim 10^6$ . Substituting the observed characteristic velocity,  $v \sim 300$  km/s, one would find  $t_{diff} \sim 10^{10}$  yr  $\gg t_{age}$ .

However, the Galactic Center is not uniform. The two stellar disks and stellar clusters are observed, which significantly perturb the gravitational potential. These perturbations should strongly reduce  $t_{diff}$ . For example, if 1/30 of the core mass resides in  $N_* \sim 10$  objects with  $m_* \sim 10^3 M_\odot$  then  $t_{diff} \sim 10^8$  yr. The corresponding acquired thickness of the stellar disk is  $H/r \sim t_{age}/t_{diff} \sim 0.1$  in agreement with the observed value. A similar estimate for  $t_{diff}$  may be derived from the interaction between the two young disks (Nayakshin et al. 2005).

The eccentricities of disk stars must also diffuse with time. If the stars were born on circular orbits then  $e \sim 0.1$  are expected to develop as the disk thickens to  $H/r \sim 0.1$ . Table 1 shows that a significant fraction of the young stars in the clockwise disk have relatively large eccentricities. The data are at best marginally consistent with the hypothesis that the stars used to have circular orbits 6 million years ago, and we leave a detailed analysis to a future work. Note that the stars may have been born in a gaseous disk that was not completely circularized: the circularization time was longer than the timescale for star formation. Then the initial eccentricities  $e$  of the stars are

non-zero. Besides, the interaction of stars with the disk might have influenced  $e$  before the disk was gone.

An alternative scenario assumes that the stars were originally bound to an inspiralling intermediate-mass black hole (IMBH; Hansen & Milosavljevic 2003), so that the observed disk plane is associated with the orbital plane of the IMBH. In this scenario, the inspiralling young cluster was stripped by the tidal field of Sgr A\* and left a disk of stars with a small dispersion of orbital planes. Calculations of Levin, Wu, & Thommes (2005) show that the stripped stars can generally have eccentric orbits. However, the inspiralling cluster scenario appears to be in conflict with the observed stellar distribution in the clockwise disk (see also Paumard et al. 2006 for discussion).

AMB was supported by Alfred P. Sloan Fellowship.

## REFERENCES

- Beloborodov, A. M., & Levin, Y. 2004, *ApJ*, 613, 224 (BL04)
- Eckart, A., & Genzel, R. 1996, *Nature*, 383, 415
- Eisenhauer, F., et al. 2005, *ApJ*, 628, 246
- Genzel, R., Eckart, A., Ott, T., & Eisenhauer, F. 1997, *MNRAS*, 291, 219
- Genzel, R., Pichon, C., Eckart, A., Gerhard, O. & Ott, T. 2000, *MNRAS*, 317, 348
- Genzel, R., et al. 2003, *ApJ*, 594, 812
- Ghez, A.M., Klein, B.L., Morris, M., & Becklin, E.E. 1998, *ApJ*, 509, 678
- Ghez, A. M., Morris, M., Becklin, E. E., Tanner, A., & Kremenek, T. 2000, *Nature*, 407, 349
- Ghez, A. M., Salim, S., Hornstein, S. D, E. E., Tanner, A., Lu, J. R., Morris, M., Becklin, E. E., & Duchêne, G. 2005, *ApJ*, 620, 744
- Hansen, B. M. S., & Milosavljevic, M. 2003, *ApJ*, 593, L77
- Levin, Y., & Beloborodov, A. M. 2003, *ApJ*, 590, L33 (LB03)
- Levin, Y., & Wu, A. S. P., & Thommes, E. W. 2005, *ApJ*, in press (astro-ph/0502143)
- Nayakshin, S., Dehnen, W., Cuadra, J., & Genzel, R. 2005, *MNRAS*, in press (astro-ph/0511830)
- Paumard, T., et al. 2006, *ApJ*, in press (astro-ph/0601268)
- Reid, M. J. 1993, *ARA&A*, 31, 345
- Schödel, R., et al. 2002, *Nature*, 419, 694
- Schödel, R., Ott., T., Genzel, R., Eckart, A., Mouawad, N., & Alexander, T. 2003, *ApJ*, 596, 1015

Table 1: Positions and velocities of the clockwise disk stars in their orbital planes

Name	$\psi$	$x$	$y$	$z$	$r$	$\phi$	$v_r$	$v_\phi$	$e$
E15: [GKM98] S1-3	$0.5 \pm 2.9$	0.52	1.03	$1.88 \pm 0.40$	$2.22 \pm 0.34$	$80 \pm 3$	$-12 \pm 42$	$534 \pm 22$	$< 0.33$
E16: [GEO97] W5	$13.7 \pm 4.7$	-1.13	0.31	$0.27 \pm 0.28$	$1.23 \pm 0.09$	$164 \pm 16$	$51 \pm 187$	$608 \pm 63$	$< 0.47$
E17	$-6.9 \pm 3.8$	-0.05	-1.21	$-2.04 \pm 0.57$	$2.40 \pm 0.52$	$271 \pm 2$	$-33 \pm 34$	$429 \pm 29$	$0.28 \pm 0.13$
E18: [GEO97] W11	$-11.4 \pm 3.4$	-0.79	-1.04	$-2.35 \pm 0.67$	$2.71 \pm 0.59$	$251 \pm 7$	$274 \pm 68$	$408 \pm 45$	$0.62 \pm 0.14$
E20: GCIRS 16C	$-18.5 \pm 4.9$	1.36	0.58	$1.47 \pm 0.56$	$2.11 \pm 0.42$	$59 \pm 9$	$-70 \pm 83$	$454 \pm 48$	$0.34 \pm 0.14$
E21: [GEO97] W13	$-1.4 \pm 4.0$	-1.02	-1.20	$-2.29 \pm 0.54$	$2.81 \pm 0.50$	$252 \pm 4$	$-99 \pm 38$	$389 \pm 29$	$0.35 \pm 0.11$
E22: [GEO97] W10	$0.2 \pm 3.7$	-1.63	-0.37	$-1.08 \pm 0.40$	$2.02 \pm 0.22$	$217 \pm 11$	$148 \pm 106$	$505 \pm 45$	$0.35 \pm 0.15$
E23: GCIRS 16SW	$6.4 \pm 5.8$	1.26	-1.18	$-1.75 \pm 0.61$	$2.50 \pm 0.48$	$308 \pm 12$	$-131 \pm 85$	$398 \pm 49$	$0.42 \pm 0.16$
E24: [GEO97] W7	$-0.2 \pm 5.0$	-2.00	0.17	$-0.25 \pm 0.46$	$2.08 \pm 0.13$	$188 \pm 14$	$-36 \pm 99$	$390 \pm 43$	$0.46 \pm 0.12$
E25: [GEO97] W14	$-12.3 \pm 5.1$	-1.97	-0.60	$-1.38 \pm 0.79$	$2.58 \pm 0.57$	$216 \pm 15$	$-86 \pm 94$	$329 \pm 49$	$0.54 \pm 0.15$
E27: GCIRS 16CC	$-9.3 \pm 6.5$	2.41	0.65	$1.62 \pm 0.65$	$3.03 \pm 0.39$	$40 \pm 12$	$95 \pm 79$	$300 \pm 43$	$0.54 \pm 0.15$
E28: GCIRS 16SSE2	$0.0 \pm 3.4$	1.74	-1.79	$-2.55 \pm 0.65$	$3.61 \pm 0.48$	$305 \pm 9$	$-119 \pm 67$	$404 \pm 31$	$0.37 \pm 0.14$
E29	$-14.2 \pm 6.6$	1.19	2.20	$3.85 \pm 0.68$	$5.25 \pm 1.36$	$85 \pm 4$	$-97 \pm 49$	$252 \pm 30$	$0.51 \pm 0.13$
E30: GCIRS 16SSE1	$-4.7 \pm 3.9$	1.91	-1.63	$-2.22 \pm 0.69$	$3.41 \pm 0.52$	$310 \pm 11$	$-27 \pm 69$	$370 \pm 28$	$0.27 \pm 0.13$
E32: MPE+1.6-6.8	$6.4 \pm 6.7$	2.22	-1.38	$-1.82 \pm 0.76$	$3.25 \pm 0.47$	$321 \pm 11$	$-121 \pm 101$	$387 \pm 56$	$0.42 \pm 0.18$
E34:MPE+1.0-7.4	$1.7 \pm 7.1$	1.52	-2.26	$-3.24 \pm 0.73$	$4.40 \pm 0.81$	$297 \pm 7$	$27 \pm 47$	$313 \pm 43$	$0.33 \pm 0.16$
E35: GCIRS 29NE1	$-2.9 \pm 7.6$	-1.19	2.47	$3.59 \pm 0.72$	$4.68 \pm 0.75$	$111 \pm 6$	$29 \pm 68$	$372 \pm 48$	$< 0.59$
E36	$-1.7 \pm 4.4$	0.54	2.75	$4.23 \pm 0.68$	$5.54 \pm 0.92$	$89 \pm 2$	$45 \pm 23$	$326 \pm 29$	$< 0.38$
E38	$-1.4 \pm 6.5$	0.23	3.31	$4.16 \pm 0.64$	$6.35 \pm 0.98$	$93 \pm 3$	$60 \pm 25$	$336 \pm 40$	$< 0.68$
E40: GCIRS 16SE2	$-3.7 \pm 9.4$	3.53	-1.43	$-1.44 \pm 0.85$	$4.15 \pm 0.33$	$335 \pm 11$	$-82 \pm 95$	$365 \pm 53$	$0.40 \pm 0.19$
E41: GCIRS 33E	$16.0 \pm 9.4$	0.78	-3.74	$-4.29 \pm 0.60$	$7.85 \pm 1.65$	$283 \pm 6$	$-143 \pm 32$	$214 \pm 47$	$0.61 \pm 0.14$
E43	$-19.8 \pm 7.2$	-1.92	-3.35	$-4.07 \pm 0.71$	$7.45 \pm 1.82$	$253 \pm 7$	$16 \pm 55$	$238 \pm 32$	$0.38 \pm 0.17$
E44	$-13.3 \pm 5.9$	1.74	3.54	$4.36 \pm 0.51$	$8.14 \pm 1.58$	$86 \pm 4$	$-124 \pm 40$	$252 \pm 30$	$0.53 \pm 0.16$
E50: GCIRS 16SE3	$-5.5 \pm 4.1$	4.02	-1.39	$-1.12 \pm 0.91$	$4.49 \pm 0.26$	$340 \pm 10$	$-121 \pm 83$	$308 \pm 37$	$0.41 \pm 0.18$
E54	$12.6 \pm 5.0$	-4.40	2.16	$2.55 \pm 1.05$	$5.75 \pm 0.76$	$144 \pm 13$	$51 \pm 72$	$282 \pm 31$	$0.33 \pm 0.16$
E56: GCIRS 34W	$1.5 \pm 4.7$	-4.86	1.91	$1.86 \pm 1.06$	$5.66 \pm 0.43$	$157 \pm 12$	$-83 \pm 79$	$323 \pm 34$	$0.38 \pm 0.16$
E57	$3.0 \pm 6.9$	5.30	0.30	$1.78 \pm 1.15$	$5.79 \pm 0.62$	$24 \pm 11$	$-33 \pm 65$	$240 \pm 35$	$0.45 \pm 0.16$
E61: GCIRS 34NW	$10.3 \pm 5.5$	-4.48	3.42	$3.70 \pm 0.97$	$7.33 \pm 1.04$	$132 \pm 10$	$-4 \pm 63$	$283 \pm 29$	$< 0.46$

Positions are offsets from Sgr A\* .

$x, y, z, r$  are in units of  $10^{17}$  cm,  $v_r$  and  $v_\phi$  — in km/s,  $\psi$  and  $\phi$  — in degrees.

In order to express distances in arcseconds one should divide  $x, y, z, r$  in the table by 1.20.